Supplemental FIG. 1: Gastric paraffin sections from 12-week old *H. pylori*-infected TG mice were stained with the anti-P-STAT3 antibody and a biotin-conjugated secondary antibody (A). Arrows in A point to P-STAT3 positive cells. B: magnified window depicting P-STAT3 positive nuclei. Size bar, 50 μ in A, 20 μ in B. Results similar to those depicted in the figure were observed in at least two other separate animals.

Supplemental FIG. 2: TFF2 and MUC6 expression in *helicobacter*-infected WT- and TG-mice. TFF2 (A) and MUC6 (B) mRNA signals in WT mice were compared to those detected in TG-mice in the presence and absence of *H. pylori* (HP) using QRT-PCR and displayed as fold-increase over WT negative controls. Values are shown as means ± SE, n=4. * $p < 0.05$; N.S., non significant.

Supplemental FIG. 3: Frozen sections from *H. felis*-infected BMP-4$^{\beta\text{-gal}/+}$mice were stained with H&E (A) and with anti-F4/80 primary antibodies and Alexa 594-conjugated secondary antibodies (red) (B). The boxed areas mark matching fields of the sections with inflammatory infiltrates.

Supplemental FIG. 4: Frozen sections from *H. felis*-infected BRE-β-gal mice were stained with H&E (A) and with anti-H^+,K^+-ATPase α-subunit primary antibodies and FITC-conjugated secondary antibodies (B).

Supplemental FIG. 5: Gastric paraffin sections from two separate 12-week old *H. pylori*-infected wild type mice were stained with the anti-p-Smad1-5-8 antibody and a biotin-conjugated secondary antibody (A and B). Arrows in A and B point

to p-Smad1-5-8 positive cells. Results similar to those depicted in the figure were observed in at least two other separate animals.

Supplemental FIG. 6: Effect of BMP-4 on cytokine release from isolated and cultures mouse dendritic cells. IL-12 (A) and IL-23 (B) content in cultures of dendritic cells treated with either LPS (1 μg/mL) or BMP-4 (20 ng/mL), alone, and in combination, was measured by ELISAs. IFN-γ (C) and IL-17 (D) content in cultures of splenocytes that were cultured with dendritic cells treated with either LPS or BMP-4 alone, and in combination, was measured by ELISAs. N.S., non significant. N.D., not detected.

Supplemental FIG 7: Effect of Noggin on BMP-4- and TGF-β-stimulated Smad phosphorylation. Expression of P-Smad1 (A), P-Smad2 (B) and GAPDH in lysates from parietal cells treated with either BMP-4 (A) or TGF-β (B) in the presence and absence of Noggin, was studied by western blots with anti-P-Smad1, anti-P-Smad2 and anti-GAPDH antibodies.

Supplemental FIG. 8: Inhibition of basal and TNF-α-stimulated IL-8 gene expression by BMP-4 in human gastric AGS cells. IL-8 mRNA abundance in AGS cells stimulated with TNF-α (10 ng/mL) in the presence and absence of BMP-4 (20 ng/mL) alone or in combination with LDN-193189 (100 nM), was measured by QRT-PCR. Values are shown as means ± SE, n=3. * and # $p < 0.05$ versus basal, ## $p < 0.05$ versus TNF-α-stimulated IL-8 gene expression, ** $p < 0.05$ versus BMP-4-inhibited IL-8 gene expression, ### $p < 0.05$ versus BMP-4 inhibited IL-8 gene expression in the presence of TNF-α.

Supplemental FIG. 9: Inhibition of basal and TNF-α-stimulated IL-8 release by BMP-4 in human gastric AGS cells. IL-8 content in cultures of AGS cells treated with either TNF-α (10 ng/mL) or BMP-4 (20 ng/mL) alone, and in combination, was measured by ELISA. Values are shown as means ± SE, n=3. * $p < 0.05$.

Supplemental FIG.10 : Effect of BMP-4 on TNF-α-stimulated NF-κB activation. A: Aliquots of IL-8 and GAPDH mRNAs extracted following exposure of either Ad.dom.neg.IκB- or Ad.CMV-β-gal-transduced canine parietal cells to TNF-α, were measured by Northern blots. B: IκBα phosphorylation in lysates from parietal cells stimulated with TNF-α for 5 and 30 min, in the presence and absence of BMP-4, was examined by western blot assays using antibodies recognizing phosphorylated forms of IκBα. Similar results were obtained in experiments with two other separate parietal cell preparations. C: IκBα degradation in lysates from parietal cells stimulated with TNF-α in the presence and absence of BMP-4 was examined by western blot assays using antibodies recognizing IκBα irrespective of its phosphorylation state. D: AGS cells were transfected with the plasmids 2XNF-κB-Luc and Renilla-Luc and treated with TNF-α (10 ng/ml), in the presence and absence of BMP-4 (20 μg/ml). Data are expressed as fold change over control, mean ± S.E. RLU, relative light units.

Supplemental Material

Supplemental Methods:

Mice. H/K-noggin transgenic mice were previously described (17). BRE-β□gal mice (28) were obtained from L. Oxburgh (Maine Medical Center Research Institute). BMP-4$^{\beta\square gal/+}$ mice (29) were obtained from B. Hogan (Duke University). Specific-pathogen-free female C57BL/6 mice aged 8 to 10 week were purchased from Jackson Laboratory (Bar Harbor, ME). Animals were housed in the animal maintenance facility at the University of Michigan. All animal experiments were approved by the University of Michigan Animal Care and Use Committee.

***Helicobacter pylori* and *H. felis* culture and infection.** Three-month old wild type C57BL/6 mice, BRE-β□gal mice, BMP-4$^{\beta\square gal/+}$ mice and noggin transgenic mice were orally inoculated with overnight broth cultures of approximately 10^8 cfu of either *H. pylori* (SS1) or *H. felis* organisms (30,31). Both infected and non-infected animals were sacrificed eight to twelve weeks after inoculation. QRT-PCR with specific primer pairs for *Ure A* and for the 16S rRNA species specific for *Helicobacter* (30) was used to document infection of the gastric mucosa.

***H. pylori* LPS isolation.** *H. pylori* LPS was isolated from the SS1 strain using the Westphal method as previously described (30,31).

Primary cell culture. For preparation, isolation and culture of the primary gastric cells we utilized modifications the methods of Soll et al, as previously described (16).

Generation of bone marrow-derived DCs. Briefly, erythrocyte-depleted murine bone marrow cells were cultured in complete medium with 10 ng/mL GM-CSF and 10 ng/mL IL-4 at 1 x 10^6 cells/mL. On day 6, non-adherent DCs were harvested by vigorous pipetting and enriched by gradient centrifugation using the OptiPrep density solution (Sigma) according to manufacturer's instruction. The low-density interface containing the DCs was collected by gentle aspiration. The recovered DCs were washed twice with RPMI-1640 and cultured in complete medium with GM-CSF (10 ng/mL). In some studies, LPS-pulsed DCs were co-cultured with syngeneic naïve splenocytes that were isolated by flushing the spleens with RPMI-1640 (DC to splenocyte ratio of 1:10), for 72 h (32,33).

ELISA. Supernatants of cultures of human AGS cells, mouse DCs and of co-cultures of mouse dendritic cells/splenocytes were collected and stored immediately at -20℃. ELISA kits for mouse IL-12p7 0, IL-23, IL-17α and IFN-γ and for human IL-8 (R&D Systems, Minneapolis, MN) were used according to the manufacturer's instructions.

QRT-PCR analysis. QRT-PCR was performed according to previously published methods (17) using primer sequences and protocols that were obtained from commercially available sources (SA Biosciences Corp., Frederick, MD).

Histochemical analysis and image acquisition. Tissue fixation, generation of paraffin sections, c□y□□□□□□□□□□□, β-galactosidase staining (28) and immunostaining were performed according to previously published methods (17).

Frozen sections were stained with the following primary antibodies: anti-β-galactosidase (1:1500) (gift from James Douglas Engel, Department of Cell and Developmental Biology, University of Michigan), anti-actin, α-smooth muscle-Cy3 (1:500) (Sigma, St Louis, MO), anti-F4/80 (1:100), anti-CD19 (1:50) (AbD Serotec, Raleigh, NC), FITC-conjugated-anti-CD3 (1:100), FITC-conjugated-anti-CD11c (1:100) (BD Pharmingen, BD Bioscience, Bedford, MA and Biolegend, San Diego, CA), FITC-conjugated-anti-MPO (1:50) (Abcam, Cambridge, MA) and anti-H_+/K_+-ATP-ase α-subunit (1:500) (Medical and Biological Laboratories, Nagoya, Japan). Paraffin sections were stained with the following primary antibodies: anti-phosphorylated serines 463 and 465 of Smad1 (1:100), anti-phosphorylated tyrosine 705 of Stat3 (1:400) (Cell Signaling, Beverly, MA), anti-Ki67 (1:500) (Novocastra, Newcastle upon Tyne, UK) and anti-Proliferating Cell Nuclear Antigen (PCNA) (1:400) (Dako, Corporation, Carpinteria, CA). For immunohistochemistry with detection with diaminobenzidine as substrate, slides were rinsed and subsequently treated with biotin-conjugated secondary antibodies (1:200) (Vector Laboratories, Burlingame, CA) for 30 min at room temperature. To visualize biotin staining, the Vectastain Elite ABC kit was used (Vector Laboratories), followed by counterstaining with hematoxylin. For immunofluorescence analysis, FITC-donkey anti-rabbit (1:100), Alexa 594-donkey anti rat (1:500) and Alexa 555-donkey anti-rabbit (1:500), secondary antibodies were used (Molecular Probes, Eugene, OR). ProLong Gold Antifade reagent with DAPI (Invitrogen, Carlsbad, CA) was used for nuclear counterstain and mounting medium. Control experiments were performed by incubating the

slides in the presence of the secondary antibodies without the primary antibodies (data not shown). Both paraffin and frozen sections were also stained with hematoxylin and eosin (H&E) to visualize cellular morphology (17). Visualization of slides was performed with either a Zeiss LSM 510 version 3.2, confocal microscope for the experiments with the anti-F4/80 and anti-CD11c antibodies, or with a Nikon Eclipse E 800 fluorescence microscope for all other studies. For histologic scoring of gastritis, sections from the stomachs of four separate animals from each of the four treatment groups were examined and scored as previously described (33,34). Slides containing sections of well-oriented gastric glandular mucosa were examined in a blinded fashion. Only fields that contained full-thickness gastric mucosa that was oriented perpendicularly were analyzed. All well-oriented fields were scored. Each field was scored separately for the presence or absence of neutrophilic and mononuclear cell infiltration, gastritis and epithelial metaplasia/dysplasia and the score was expressed as a percent affected fields (33,34). In addition, the severity of the changes was graded using a scale from 1 (mild) to 3 (severe). To score the extent and severity of dysplasia, individual microscopic fields were examined for the presence of glandular dysplasia (score =1), defined as dilation, irregularity, disorganization of glands, cellular atypia (score = 2), defined as anisocytosis/karyosis, loss of polarity, abnormal shape, piling up, altered differentiation, and gastric intraepithelial neoplasia (score =3), defined as well-demarcated foci of loss of differentiation with features of cellular atypia. Each field was scored, and the final score was calculated as a weighted average of all fields (sum of the number of fields for

each score x the score, divided by the total number of fields).

Northern blots. Northern blots were performed according to previously published methods (16). The primary cells were lysed with TRIzol (Gibco BRL, Grand Island, NY) according to the manufacturer's instructions. Northern blot hybridization assays were performed as previously described (16) using specific canine IL-8 and human glyceraldehyde-3-phosphate dehydrogenase (GAPDH) cDNA probes.

Western blots. Western blots were performed according to published reports using previously described methods (16,17). For the phospho-STAT-3, phospho-IκB-α, p□□□□□□□□□□□□□ and phospho-Smad2 western blots we used antibodies recognizing phosphorylated tyrosine 705 of STAT3, phosphorylated serine 32 of IκB-α, phosphorylated serines 463 and 465 of Smad1 and phosphorylated serines 465 and 467 of Smad2 (1:1000) (Cell Signaling, Beverly, MA). Non-phosphorylated forms of IκB-α were detected by western blots with anti- IκB-α antibodies (1:200) (Santa Cruz Biotechnology, Santa Cruz, CA). Control blots were performed using anti-GAPDH antibodies (1:1000) (Chemicon International, Temecula, CA).

AGS cells culture. AGS cells (human gastric adenocarcinoma cells) were purchased from ATCC (Manassas, VA, USA) and cultured in Dulbecco's modified Eagle's medium (DMEM) with 10% fetal bovine serum (FBS).

Adenoviral vectors. The adenoviral vector expressing a mutated IκB that acts as a repressor of NF-κB (Ad.dom.neg.IκB), and the control adenoviral vector expressing the β-galactosidase enzyme under the control of the CMV promoter (Ad.CMVβ-gal) were previously described (supplemental reference 1). The recombinant adenoviruses were amplified and purified as previously described (supplemental reference 1).

Luciferase assays. Subconfluent AGS cells were transfected with the 2κB-luciferase reporter plasmid (supplemental reference 2) and the Renilla-Luc control plasmid. 2κB-luciferase was obtained from E. Burstein (University of Texas, Southwestern Medical Center). Transfections and luciferase assays were carried out using the Promega Luciferase Assay System according to the manufacturer's instructions and previously published techniques (supplemental reference 2).

Supplemental Results:

We investigated the possible mechanisms responsible for BMP-mediated inhibition of IL-8 gene expression. According to the literature, the IL-8 gene is under the control of the NF-κB, MAPK and JNK signal transduction pathways (26). In a series of experiments with an adenoviral vector expressing a NF-κB inhibitor (supplemental reference 1), we confirmed that, in the canine cells, the NF-κB signal transduction pathway regulates both basal and TNF-α□stimulated IL-8 gene expression (supplemental fig. 10A). In contrast, inhibitors of both JNK and MAPK had no significant effect on the expression of the IL-8 gene, (data not

shown). This latter observation was in agreement with previous reports from our laboratory that indicated that TNF-α has negligible effects on both MAPK and JNK activation in the parietal cells (supplemental reference 3). We then investigated if BMP-4 regulates the process of IκBα phosphorylation and degradation, a signaling mechanism that leads to NF-κB activation (26,supplemental reference 4). In these studies we observed that BMP-4 had no effect on both basal and TNF-α-stimulated IκBα phosphorylation and degradation in both canine (supplemental fig. 10B and C) and AGS cells (data not shown). Moreover, BMP-4 failed to inhibit basal and TNF-α-stimulated luciferase activity in AGS cells transfected with a NF-κB-luciferase reporter plasmid (supplemental fig. 10D). Thus, BMP-4 appears to inhibit IL-8 gene expression through mechanisms that do not involve IκB-regulated NF-κB activation.

Supplemental References:

1. Pausawasdi N, Ramamoorthy S, Crofford LJ, et al. Regulation and function of COX-2 gene expression in isolated gastric parietal cells. Am J Physiol Gastrointest Liver Physiol 2002;282:G1069-1078.

2. Burstein E, Hoberg JE, Wilkinson AS, et al. COMMD proteins, a novel family of structural and functional homologs of MURR1. J Biol Chem 2005;280:22222-22232.

3. Nagahara A, Wang L, Del Valle J, et al. Regulation of *c-jun* n-terminal kinases in isolated canine gastric parietal cells. Am J Physiol 1998;275:G740-G748.

4. Karin M, Greten FR. NF-κB linking inflammation and immunity to cancer development and progression. Nature 2005;5:749-759.

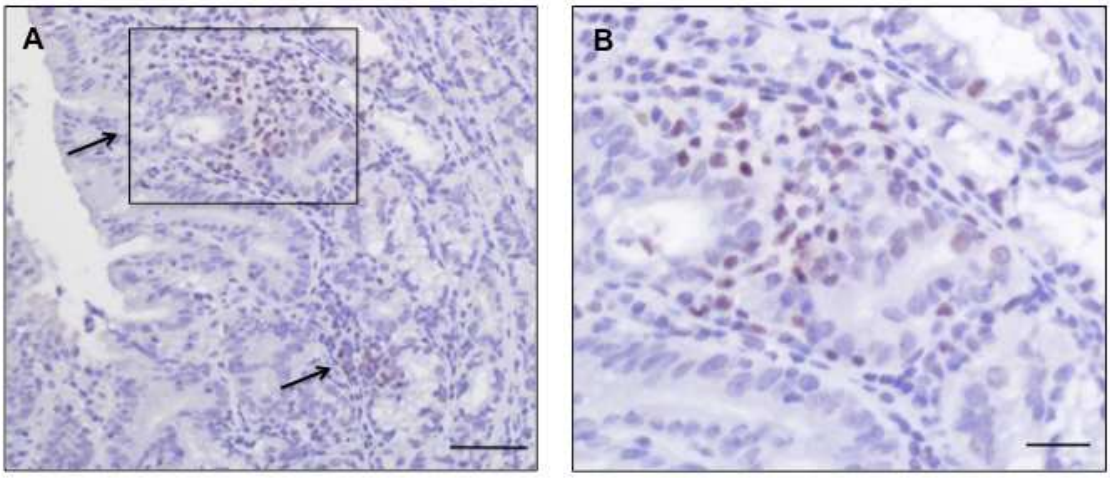

A

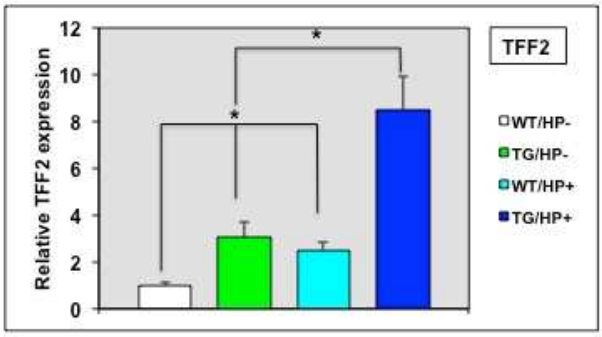

B